



**CHALMERS**  
UNIVERSITY OF TECHNOLOGY



## **Characterization and control of modetuned reverberation chamber**

Bachelor's thesis in electrical engineering

LUKAS RIDDERSTRÅLE

Institutionen för Elektroteknik  
CHALMERS TEKNISKA HÖGSKOLA  
Göteborg, Sverige 2024

BACHELOR'S THESIS 2024

**Characterization and control of modetuned reverberation chamber**

LUKAS RIDDERSTRÅLE



Institutionen för Elektroteknik  
CHALMERS TEKNISKA HÖGSKOLA  
Göteborg, Sverige 2024

**Characterization and control of modetuned reverberation chamber**  
**LUKAS RIDDERSTRÅLE**

© LUKAS RIDDERSTRÅLE 2024

Supervisor: ZACKARY CHIRAGWANDI, EMC SERVICES  
TEEMU PALMÈR, EMC SERVICES

Examiner: THOMAS HAMMARSTRÖM, CHALMERS

Bachelor's Thesis 2024  
Institutionen för Elektroteknik  
CHALMERS TEKNISKA HÖGSKOLA  
SE-412 96 Göteborg  
Telephone +46 (0)31 772 1000

Cover: The reverberation chamber and the Stepper motor turning it.  
Möln dal, Sweden 2024

Preface:

This project was performed as a bachelor's thesis in electro engineering, at Chalmers University of Technology. It was done at EMC SERVICES at their office in Möln dal.

Firstly I want to thank my supervisor at EMC SERVICES Zackary Chiragwandi and his replacement Teemu Palmér. Who took the time to plan out and execute this project. I also want to thank all of my other colleagues at EMC SERVICES for always helping me when it was needed.

And of course I want to thank my supervisor and examiner Thomas Hammarström at Chalmers and lastly i want to give thanks to Ramiro Serra from EINDHOVEN UNIVERSITY OF TECHNOLOGY who provided important theories of the understanding of the chamber characterization.

Lukas Ridderstråle january 2024, Gothenburg

## Abstract

Modetuned Reverberation chambers (RVC) are widely employed in Electromagnetic Compatibility (EMC) testing. The main use for the chamber is to create a highly uniform and isotropic magnetic field environment.

They offer an enhanced control over the field distribution by creating specific resonant modes. This project aims to characterize the performance of an RVC in the purpose of EMC testing applications. Going over theoretical principles, fundamental concepts of mode stirring and tuning including stirrer design and mechanisms.

It further evaluates the effectiveness of mode tuning in achieving a high field strength using relatively low power output. Comparing the experimental results with theoretical predictions using the preexisting reverberation chamber at the EMC lab at EMC Services.

The need for an automatic steering module to improve functionality and ease of usage was constructed using an Arduino microcomputer controlling a stepper motor with some added features for display of orientation and functionality for different rotation techniques to fit different EMC standards.

## Sammanfattning

Modväxlande kammare (RVC) är en testmiljö för elektromagnetisk kompatibilitetstestning (EMC). Huvudsyftet med kammaren är att skapa en uniform isotropisk magnetfälts miljö, detta ger en mer precis kontroll över fält fördelningen genom att skapa olika resonans lägen. Detta projekt fokuserar på att karakterisera prestandan i en RVC för relevanta EMC-testmetoder genom att använda teoretiska principer och grundläggande egenskaper av modväxling. Effektiviteten av modväxlingens förmåga att uppnå hög fältstyrka med låg utgångseffekt kommer utvärderas och jämförelser utförs mellan hypoteser/teoretiska beräkningar och experiment utförd i kammaren i EMC labbet på EMC-Services. Behovet av att konstruera en styrmodul för att automatisera testet och öka funktionaliteten så konstruerades en styrkrets med en arduino som styr en stegmotor samt andra funktioner så som steg display och olika rotations lägen.

# Table of content

Terminology	1
<b>1 INTRODUCTION</b>	<b>2</b>
1.1 Background	2
1.2 Aim	2
1.3 Boundaries	3
<b>2. Theoretical Background</b>	<b>4</b>
2.1 Modetuned Reverberation chamber	4
2.1.1 Calibration Factor	6
2.1.2 Quality factor	7
2.2 Hardware	9
<b>3. METHOD</b>	<b>12</b>
3.1 Initial work	12
3.2 Stirring control	12
3.3 Test procedure and test setup	14
<b>4 Results</b>	<b>15</b>
4.1 Chamber specifications	15
4.2 Quality Factor	16
4.3 Calibration factor	19
4.4 Field Homogeneity	20
4.5 Programming Python script	21
4.6 Arduino circuit	22
4.7 Programming Arduino	25
<b>7. Conclusion</b>	<b>26</b>
7.1 implementation of stepper motor control	26
7.2 Development of control Program	26
7.3 Analysis according to standards	27
<b>References</b>	<b>28</b>

## Terminology

RVC - Reverberation Chamber

EMC - Electromagnetic Compatibility

PWM - Pulse Width Modulation

RF - Radio Frequency

EUT - Equipment Under Testing

# 1 Introduction

## 1.1 Background

EMC Services was in the possession of an unused RVC, which required both modification and characterization for it to be useful in EMC testing procedures. This project is built on rendering the RVC operational for EMC testing and is performed at EMC Services in Mölndal.

It presents the possibility of conducting EMC tests in a high field strength environment for smaller test objects using a fraction of the power. Additionally this conserves customer time and financial resources by not needing to book a full semi-anechoic test chamber, this also allows EMC Services to have more customers testing simultaneously.

## 1.2 Aim

The purpose of this project is to study and complete an existing RVC.

1. It shall be provided with stepper motor control for the stirrer with incremental and continuous rotation. A program to control the test equipment shall also be developed and implemented to reduce test time.  
If needed to fulfill the project objectives a new stirrer shall be constructed.
2. The chamber shall be analyzed in respect to the performance according to the standards MIL461G[1] and RTCA DO160G[2] to determine the frequency range, field uniformity, Q-value and power effectivity. These activities can be summarized in the following.
  - Implementing an automatic stirrer with incremental and continuous rotation.
  - Implementing a program to connect and control all test equipment.
  - Analyze the RVC in respect to the standards.
  - Determine a reasonable frequency range.
  - Measure the RVC's field uniformity, Q-value and correlation to power output.

## 1.3 Boundaries

The project was undertaken with the timescope limited to 15 ECTS credits, necessitating careful consideration to strike a balance between fulfilling the criteria outlined in points 1 and 2, while ensuring that the workload remained within the expected boundaries. Given the pre-existence of the RVC, the majority of construction efforts were directed towards the refinement of the stirrer controller thus optimizing resource allocations.

However, due to the chamber's deviation from the prescribed dimensions outlined in industry standards, it may not fully satisfy all requirements. Consequently, its utilization will be guided by our experience and tailored to align with the specific requests of the customer.

This project's timeline extended beyond initial projections due to an increase in the numbers of customers at EMC Services during the project's duration and an unfortunate streak of sicknesses.

Furthermore, an unexpected change in supervisors caused further delay.

## 2. Theoretical Background

### 2.1 Modetuned Reverberation chamber

A modetuned Reverberation chamber is an enclosure used for electromagnetic field measurements and EMC testing.

An RVC is designed to provide a well-defined and uniform electromagnetic environment for electronic devices.

Its purpose is to generate a highly reflective (reverberant) cavity to verify the electromagnetic performance of an electronic device can handle electromagnetic interference without issues in their intended scenarios.

The reflectivity of the chamber allows the electromagnetic waves to bounce around inside the cavity creating a uniform field.

Mode-tuning is the process of adjusting the physical dimensions and properties inside the cavity to control the specific electromagnetic modes within. By turning the tuner the distribution of the electromagnetic field is changed to get a complete uniform field in the entirety of the chamber. This ensures the environment remains consistent allowing for repeatable testing results.

The equipment tested in the chamber is tested for their susceptibility of electromagnetic interference from other devices.

The chamber utilized at EMC Services has the following dimensions, Width = 80cm, Height = 150cm, Length = 100cm.

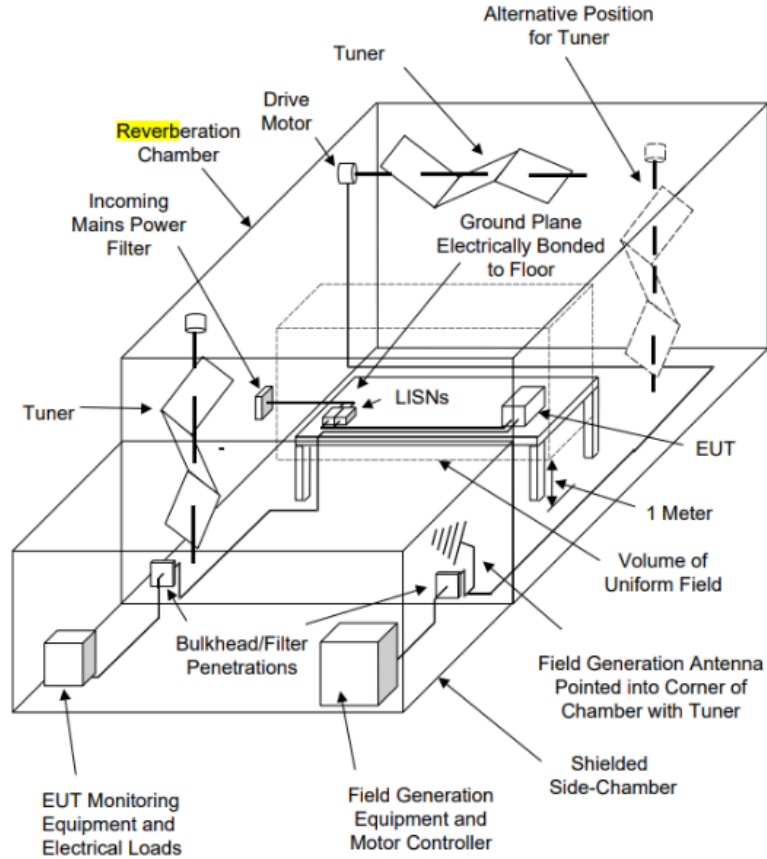


Figure 2.1.1: Mode tuned RVC taken from MIL-STD-461G [1]

The following formula determines the number of possible modes (N) which can exist at a given frequency, if N is less than 100 the chamber is unfit for the given frequency.[1]

$$N = \frac{8\pi}{3} \cdot abc \cdot \frac{f^3}{c^3}$$

Eq.(1).

where

a,b,c are the chamber internal dimensions in meters.

f is the frequency in Hz

c is the speed of the wave propagation\*

\*in this case it is considered equal to the speed of light ( $3 \times 10^8$  m/s )

Table 2.1: Required minimum number of tuner positions for a RVC [1]

Frequency Range (MHz)	Tuner Positions
200 - 300	50
300 - 400	20
400 - 600	16
Above 600	12

### 2.1.1 Calibration Factor

The calibration factor is a correction factor used to account for variations in the chamber's characteristics and performance.

Adding an Equipment under test (EUT) in this environment introduces uncertainties and variations in expected results thus the calibration factor is used to adjust measured data to compensate for these variations improving the accuracy of the test. [1]

$$\text{calibration factor} = \sqrt{\frac{\left(\frac{E_{x-max} + E_{y-max} + E_{z-max}}{3}\right)^2}{P_{forward}}} V/m \text{ (for one watt)}$$

Eq. (2).

Where

$E_{x-max}$ ,  $E_{y-max}$ ,  $E_{z-max}$  are the maximum field strength measured at that axis.

## 2.1.2 Quality factor

The quality factor, referred to as Q is the ratio of energy stored in a system compared to the energy dissipated per cycle. This concept is usually associated with resonant circuits such as RF applications

The higher the Q factor the more efficient the system is, indicating a lower rate of energy dissipation relative to the oscillation frequency.

The dominant loss for an empty cavity is due to non-perfectly conducting walls; additional losses come from the stirrer, antenna, and EUTs.

Knowing the chambers Q factor gives an estimation of the mean field strength resulting from a given input power.

There is a trade-off in the chamber design when assessing Q-factor. The larger the Q-factor is the higher the field strength that could be achieved. On the other hand a high Q-factor leads to narrower bands of excitation and thus lesser number of modes contributing to the total field, this will influence the field uniformity and therefore good tuning conditions would hardly be achieved.

### Theoretical Q

The basic definition of Q is

$$Q = \omega \cdot \frac{\text{Energy Stored}}{\text{Power Loss}} = 2\pi \cdot \frac{\text{Energy Stored}}{\text{Energy Dissipated per cycle}} \quad \text{Eq.(3)}$$

Where

$\omega$  is defined to be the angular frequency of the system

Energy stored ( $W_s$ ) and power loss ( $P_d$ ) are properties of a system.

$$W_s = \frac{1}{2} \int \int \int_V D \cdot E \, dV = \frac{1}{2} \epsilon \int \int \int_V |E|^2 \, dV$$

And since  $P_d$  equals the net input power  $P_{in}$

$$Q = \frac{\omega \epsilon}{2P_{in}} \int \int \int_V |E|^2 \, dV$$

In order to calculate this, all losses must be considered such as absorptions, leakage etc. In practice this is not possible due to the complexity of the parameters.[\[3\]](#)

### Practical Q

Instead of using the basic definition a Practical Q-factor or composite Q-factor is presented as  $\tilde{Q}$ . [3]

$$\tilde{Q} = \left\langle \frac{1}{Q} \right\rangle = \frac{3V}{2\mu_r \delta_s A} \cdot \frac{1}{\left[ 1 + \frac{3\lambda}{16} \left( \frac{1}{a} + \frac{1}{b} + \frac{1}{d} \right) \right]}$$

Eq.(4).

Where

V = chamber volume,  
A = the inner surface  
 $\delta_s$  = the skin depth of the metal defined by

$$\delta_s = \sqrt{\frac{\rho}{\pi f \mu_r \mu_o}}$$

Where

$\rho$  = resistivity  
 $\mu_r$  = relative permeability  
 $\mu_o$  = permeability of vacuum

The practical Q can also be further simplified considering in practical chambers, the values for the chamber dimensions a,b,d are large enough to obtain the usual operational frequency.

$$\tilde{Q} \approx \frac{3V}{2\mu_r \delta_s A}$$

Eq.(5).

A statistical model for Q using the basic definition and performing some simplifying assumptions found in [4] gives us.

$$Q = \frac{\omega \varepsilon \bar{E}^2 V}{2P} = \frac{3\omega \varepsilon \sigma^2 V}{P}$$

Eq.(6).

Where

V = is the chamber volume  
P = is the net input power  
 $\sigma^2$  = is an estimator of the electric field standard deviation over an ensemble of stir states.  
 $\omega$  = is the angular frequency  
 $\varepsilon_o$  = is the permittivity of vacuum

## 2.2 Hardware

### **HARDWARE COMPONENTS**

The following components were used to complete this project

- Arduino UNO R3 board SMD
- Luxorparts USB 2.+ a/B 0.5m
- Nema 17 stepper motor MOT54/SP
- Fasizi L298N Dual H Bridge stepper motor driver card for arduino
- 10k $\Omega$  resistors
- Two seven segment displays
- Three switches
- DC power unit
- RVC (Width = 80cm, Height = 150cm, Length = 100cm)

### **TEST EQUIPMENT**

- SMP02 MICROWAVE SIGNAL GENERATOR Rohde and Schwarz
- Ar field probe fp7018
- Powermeter NRVD Rohde and Schwarz

## Microcontroller

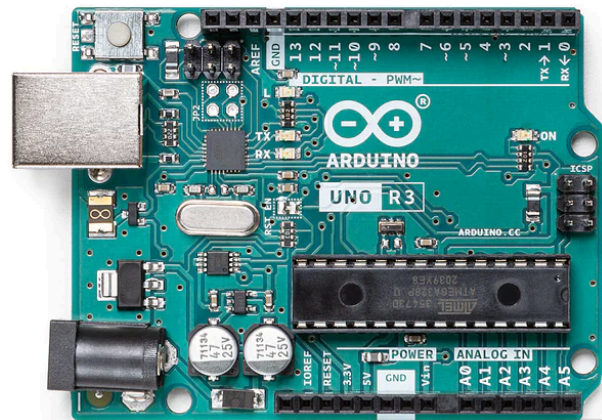


Figure 2.2.1: Arduino UNO R3 SMD

The microcontroller was an Arduino UNO R3 SMD.

Arduino uno is a widely used user-friendly open source microcontroller with an easy to understand programming environment in the software Arduino IDE.

By being open source it means access to extensive documentation, tutorials and beginner friendly code.

This product supports an extensive amount of libraries that simplifies the implementation of more advanced features needed such as acceleration and microstepping without needing complex coding.

Having multiple digital and analog pins that are easy to program to interface with stepper motor driver integrated circuits such as the L298N stepper motor driver.

Having the ability to manage several circuits simultaneously makes it perfect for the purpose of this project. [5]

## Stepper motor driver card

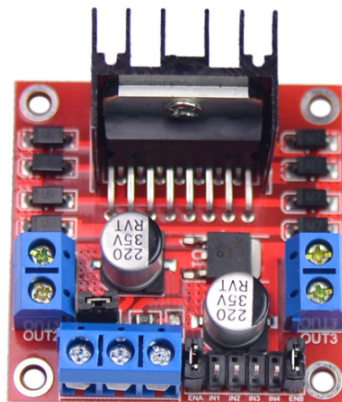
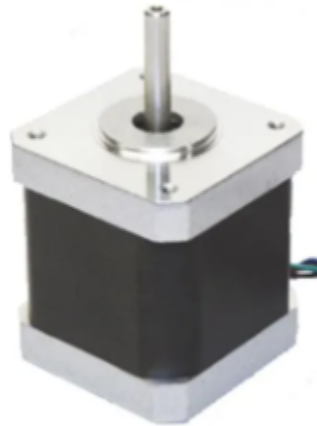


Figure 2.2.2: L298N dual H-Bridge

The L298N is a dual H-bridge integrated circuit, perfect to use as a stepper motor driver. Built to control the speed and direction of two DC step motors or one bipolar stepper motor, the H-bridge is a configuration that allows forward and reverse torque perfect for its purpose. The L298N is controlled by a logic interface accepting input signals from a microcontroller and has four control inputs.

Some limitations of the L298N is its high heat generation and that it only handles 2A of current. But the performance is found sufficient and its cheap price and easy access makes up for it.[\[6\]](#)

## Stepper Motor



*Figure 2.2.3: Nema 17 MOTS4/SP Stepper motor*

The stepper motor chosen for this project was the Nema 17 MOTS4/SP for its availability, its torque and its compatibility with the stepper motor controller.

A stepper motor is a brushless open loop DC motor with precise position control.

It consists of two main components, a rotor and a stator.

When letting current flow through the coils surrounding the stator a magnetic field is generated that attracts or repels the rotor. By activating the different coils step by step in a particular order motion of the rotor can be achieved. [\[7\]](#)

[\[8\]](#)

## 3. Method

### 3.1 Initial work

A lecture by professor Ramiro Serra was taken on the basics of reverberation chambers. [\[9\]](#)

After the lecture the access to Ramiro Serra's PHD thesis on RVC was provided which gave great insight in the theoretical aspects and measurement strategies.

### 3.2 Stirring control

In order to manage the motor, a circuit was devised utilizing an Arduino Uno, L298N stepper motor driver, and a stepper motor. Throughout the developmental stages, this circuit underwent several iterations. Initially a weaker stepper motor and a different driver were employed. However, it became evident early in the process that this design lacked the requisite power to effectively rotate the stirrer. A revised iteration featuring a more robust motor and driver was designed and implemented.

Subsequently, complications emerged with the new circuit where the motor started to shake without rotation. This issue was resolved by elevating the drive current to 2.5A but came with its own problems as the L298N stepper driver could only support up to 2A, [\[6\]](#) overheating concerns surfaced during prolonged operational periods. As the driver otherwise draw 2.5A continuously, a solution was implemented where the holding torque current was disconnected and current was exclusively supplied during the active stepping process.

To create the automatic motor control, a control board was assembled, which incorporates several buttons and a switch to facilitate functionalities such as tuner resetting, stepping and step mode alteration. Furthermore, a set of 7-segment displays was integrated to provide users with a clear indication of the current tuner step position.

In order to secure the motor onto the chamber, it was necessary to construct a fixture, this served the purpose of ensuring the motor's stability and locking it to a fixed position, thereby minimizing both vibration and any unwelcome wiggling that otherwise could impact the accuracy of the rotation.



*Figure 3.2.1: Stepper motor fixture*

To ensure effective operation of the microcontroller. Code was developed to govern tuner rotation, reset functions, stepmode adjustments and illumination of the 7-segment displays.

The coding for the Arduino underwent multiple iterations to refine its functionality To accustom for the differences between the different stepper motors during the testing phase, where a strong motor was selected due to its ability to handle the torque needed to rotate the tuner, Therefore the program needed to be able to control the current more accurately.

Additionally to streamline the manual control and data reading processes further, a Python program was developed.

This program was designed to automate tasks such as setting generator frequency, monitoring output power and collecting data from the fieldprobe's X, Y, Z axes.

The gathered data was compiled into a text document for further analysis in excel.

### 3.3 Test procedure and test setup

The test procedure is based on the established electric field probe procedure for Reverberation chambers as specified in MIL-STD-461G. However, to accommodate varying requirements, the measurement program offers flexibility to conduct tests aligned with RTCA-DO160G.

The primary distinction between the two lies in the mode of measurement, where MIL-STD-461G [1] uses stepping and RTCA-DO160G [2] uses continuous rotation.

The placement of the probe is within appropriate distances from the chamber walls and tuner. This occurs at eight distinct locations within the chamber, defining a rectangular volume at the center of the cavity, serving as the target region for uniform electric field measurements. [Figure 3.3.1](#)

The test setup includes a microwave signal generator connected to a directional coupler, with a power meter connected on the directional couplers forward path. The output of the directional coupler is connected to the wall of the chamber and through to the antenna situated inside.

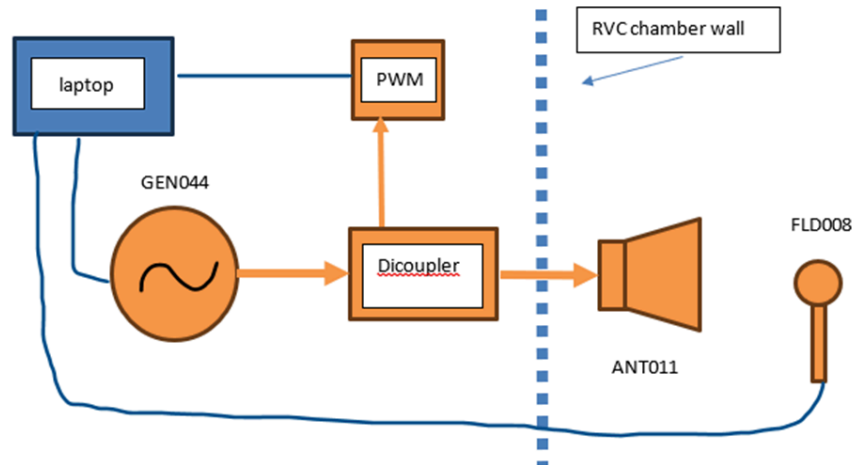


Figure 3.3.1: Full setup of chamber calibration

The generator is adjusted to inject the appropriate forward power ( $P_{forward}$ )

Without modulation into the chamber at the starting frequency of the measurement.

The tuner is rotated 360 degrees for each frequency in a logarithmic scale per decade using the minimum steps required for the given frequency given in ([Table 2.1](#)).

The tuner has to dwell at each position for a period of a minimum 1.5 times the probe response time.

The amplitude of each axis is recorded using the equation [Eq. \(2\)](#). A calibration factor is calculated for the field strength created in the cavity. [1]

## 4 Results

### 4.1 Chamber specifications

The chamber dimensions were originally configured to accommodate a minimum frequency of 1GHz.

$$\frac{0.299792458}{1 \text{ (GHz)}} \approx 0.3 \text{ m}$$

Where 0.29979248 is the wavelength in meters at 1GHz

This necessitated the measurement volume to maintain a distance of at least one wavelength from any metal surfaces, including floor, walls and stirrer in this case for the lowest frequency 1GHz with 30cm.

To verify that 1GHz was reasonable equation (1) was used with the parameters of the chamber.

$$Volume = 1.50m \cdot 0.8m \cdot 1m = 1.20 m^3$$

$$N = \frac{8\pi}{3} \cdot 1.20 \cdot \frac{1000000000^3}{3 \cdot 10^3} = 372.34$$

Given the result  $372 > 100$  verifies the functionality of the chamber for 1GHz using the parameters of Eq.(1). This frequency serves as the lower limit for tests conducted within the chamber. It was determined that the upper limit for testing would be set at 18GHz, aligning with the specifications of the test equipment.

A departure from the MIL-STD-461G [1] to be considered is that the EUT is supposed to be at least 1 meter from the closest metallic surface 0.75m for RTCA-DO160G.[2] The same is also for the antenna and field probe, this cannot be achieved due to the size of the chamber being too small.

It was determined that the number of stirring steps would be set at 16. This decision was made to provide a reasonable degree of variation between steps without overly large intervals, while also adhering to the minimum recommended steps outlined in the standard.[1].(See Figure 2.1.2)

## 4.2 Quality Factor

To calculate an estimated ideal Q the Practical Q factor formula(5) is used.

$$\frac{3V}{2\mu_r \delta_s A} = Q$$

where

$$\delta_s = \sqrt{\frac{\rho}{\pi f \mu_r \mu_o}}$$

where

$$\mu_r = 1,00002 \mu\Omega/\text{cm}$$

$$\mu_o = 4\pi \cdot 10^{-7}$$

$$\rho = 2,6548$$

Giving a skin depth between 2.6  $\mu\text{m}$  - 0.82  $\mu\text{m}$  decreasing with an increase in frequency.

Upon calculation, a theoretical / practical Q factor of the chamber volume yielded a range between 98,000 to 310,000 depending on the frequency.

It's important to note that these values are unattainable in a practical scenario with a difference of around 1-2 magnitudes in ideal settings. Nonetheless, they provide an important indication that the Q factor exhibits a trend increasing with frequency.

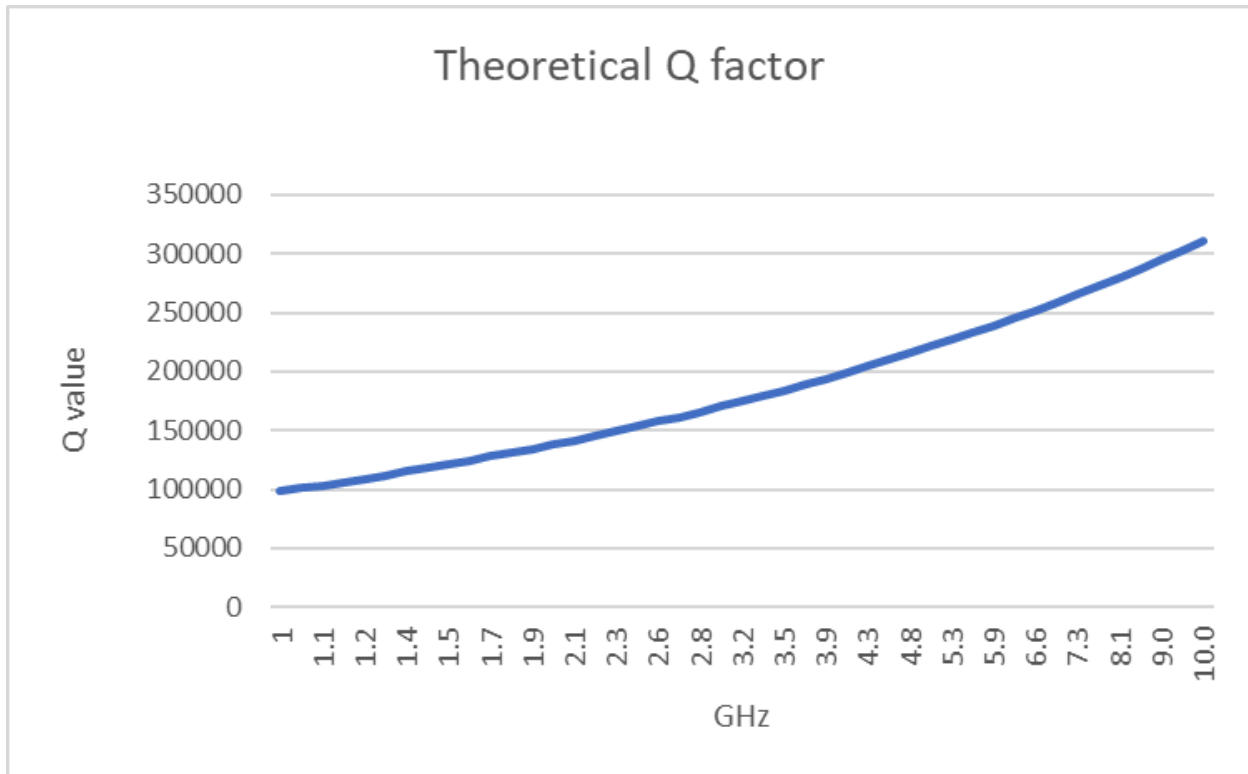


Figure 4.2.1: Theoretical Q factor over rising frequency (GHz)

Using the statistical model for Q (6)

$$\frac{3\omega\epsilon\sigma^2V}{P} = Q$$

where

$$\omega = 2\pi f$$

$$\epsilon = 8.854 \cdot 10^{-12}$$

$$\sigma^2 = \text{standard deviation of the resultant } \sqrt{x^2 + y^2 + z^2} \text{ axis}$$

P = is set at as a constant 0.03W to reduce unnecessary calculations due to being different for every position and rotation.

This was necessary to calculate for every frequency.

Taking the average of all 8 positions a Q value ranging between 74 to 729 depending on frequency is found.

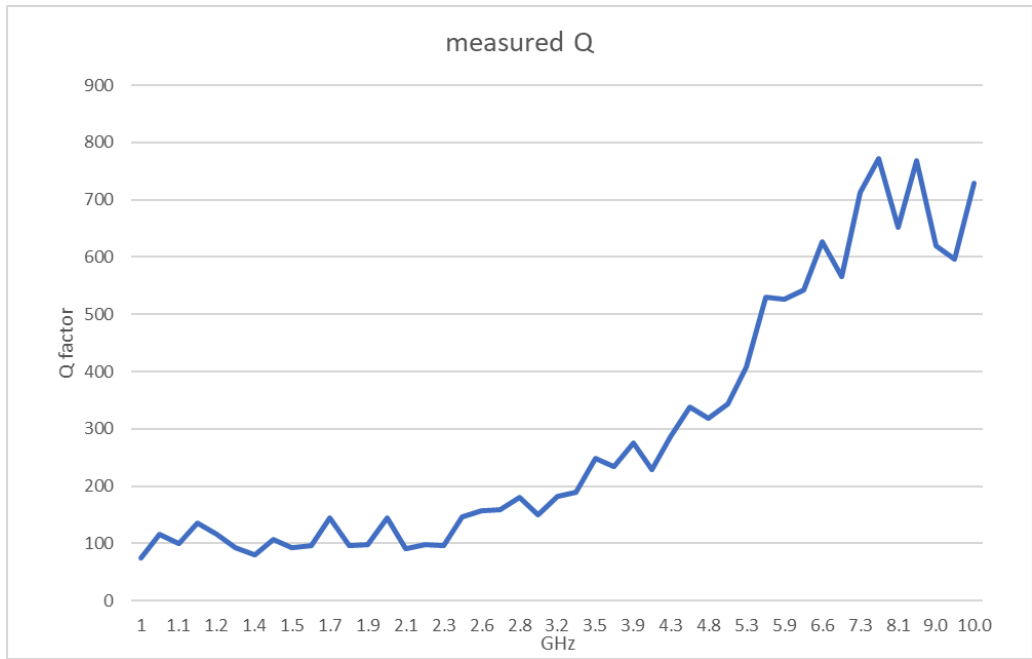


Figure 4.2.2 Measured Q factor over rising frequency (GHz)

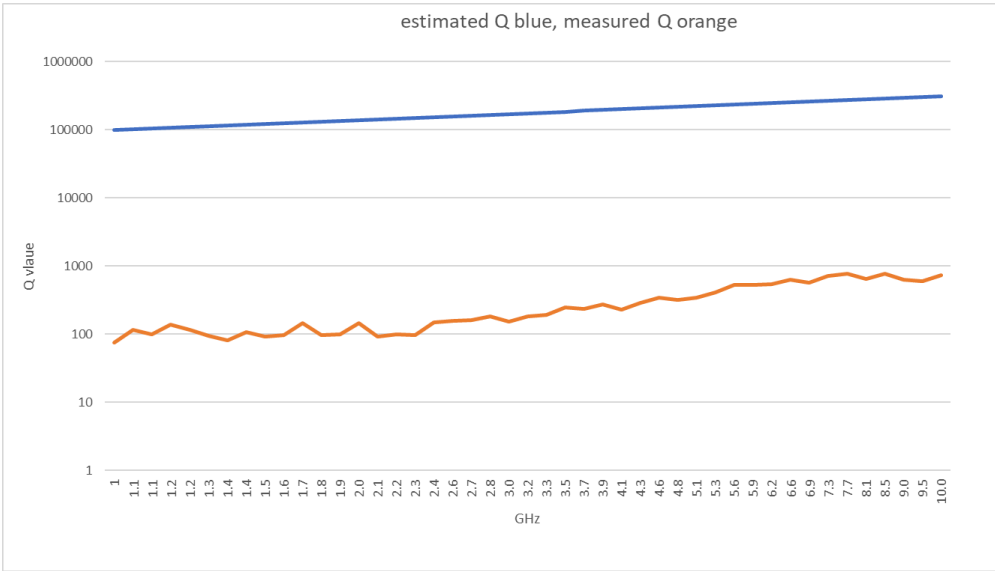


Figure 4.2.3: Comparison of the Theoretical and Statistical Q factors over frequency (GHz)

### 4.3 Calibration factor

When calculating the RVC calibration factor the formula used for MIL-STD-461G reverberation chamber calibration is used. (2)

$$\sqrt{\frac{\left(\frac{E_{x-max} + E_{y-max} + E_{z-max}}{3}\right)^2}{P_{forward}}} = \textit{calibration factor}$$

By inserting the max value of every axis on the field probe  
Combining the calibration factors from each position to create an average over each frequency

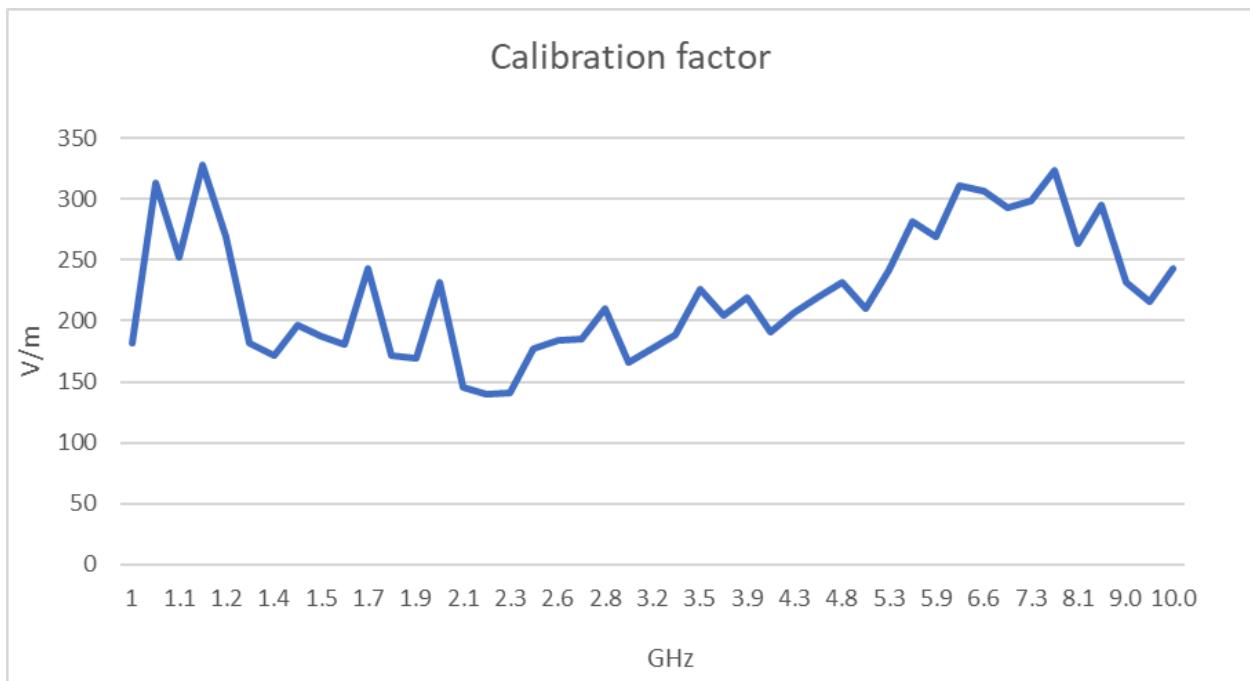


Figure 4.3.1: Calibration factor average of each position over frequency (GHz)

## 4.4 Field Homogeneity

The field uniformity in the chamber depends on a lot of different variables so to simplify it a statistical model had to be made.

The field uniformity will be calculated with the maximum value of the resultant of the field probe measurement for each position over each of the 16 steps.

Using the 8 positions in the corners of the test volume an assumption could be made that taking the value of each corner finding an average value.

$$AVG (Position_{1-8} (MAX (resultant_{step 1-16}))) = field\ uniformity \pm (max - avg) \text{ or } (avg - min)$$

$$AVG \pm \approx 20\%$$

Where

The AVG value depends on the frequency.

Which for 1 GHz gives 49.4 V/m  $\pm$  20%

Using this statistical model the result shows that the difference from the Average field to max or min value is around 20% by taking the Average of the difference for each frequency

## 4.5 Programming Python script

To receive data from the test and setting/reading the parameters of the measuring instruments a python script was written.

The instruments need to be defined properly in order to be used in the code. To be able to communicate instructions with the instruments Standard Commands for Programmable Instruments SCPI language is used.

For the case of the field probe baud rate and string length has to be set.

For the signal generator a frequency list had to be created to follow the requirements in the standards.

In Python, a script to receive data from the test instruments and setting the parameters of the measuring instruments needed to be made.

This utilized SCPI(Standard Commands for Programmable Instruments) protocol which is standardized for communicating with test and measurement instruments.

In Python the library PyVISA is necessary to be able to connect and communicate with measurement instruments since it provides SCPI capabilities.[\[10\]](#)

This is done while setting variable definitions of each instrument.

Using the .Write function a set of instructions are sent to the instruments such as.

Field probe

**CALC:AXIS? ALL,** Sets the probe to read X, Y, Z. values individually instead of the resultant

**MEAS?,** Start the measurement instruction.

Signal generator

**POW 20dbm.** Sets the output power to 20dbm (0.1W)

**OUTP:STAT ON,** enables the output signal

**FREQ + X + GHz,** sets the frequency to the value in the frequency string

Power meter

**AMPL:UNIT DBM,** sets the measurement unit to DBm

**TRG ,** sets a trigger source

A list of frequencies to cover the logarithmic stepping between 1 and 10GHz was created as an array using the library NumPy.

To be able to perform the sweep autonomous A loop containing the instructions for setting new frequency and reading both the power meter and field probe data were written and converting the string into three different float values for the probe reading was necessary to separate them.

To be able to work with the data it needed to be transferable from the script to a text document. Therefore a function to combine the readings into a .txt file was written.

## 4.6 Arduino circuit

The circuit consists of a few different sections, as seen in the figure below..

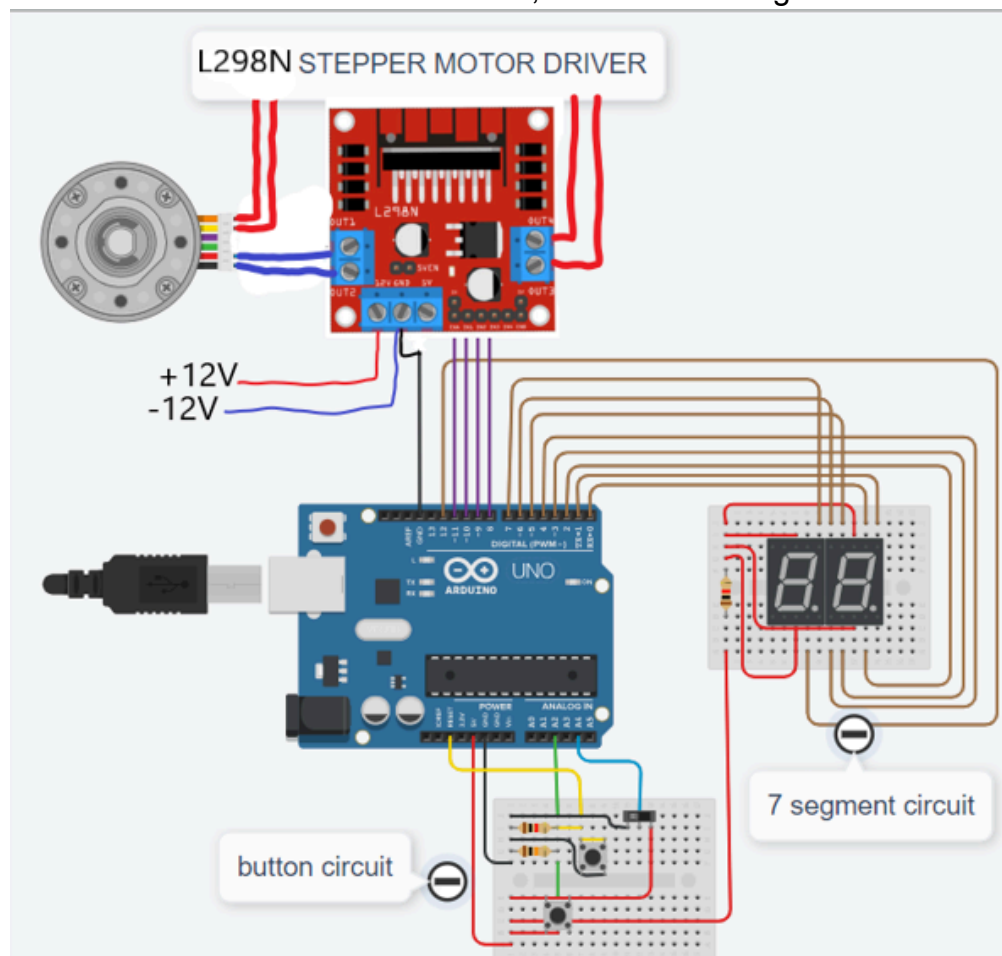


Figure 4.6.1: Picture depicting the different sections of the circuit and how they are connected.

## 7 segment circuit

The 7-segment circuit acts as a display of what step the tuner is currently using supplied by 5V from the arduino through a 1k $\Omega$  resistor feeding the 7-seg display diode. The tuner won't use more than 16 steps so only the pins necessary for 0-17 needs to be able to light up; the rest were left open.

## Button circuit

The button circuit is responsible for stepping, resetting the stirrer and changing stepping mode.

A breadboard was connected with the arduino using the arduino ground and 5V supply to send a high signal when a button was pressed down, the output of each button is connected to an input on the Arduino see [Figure 4.6.2](#)

Pull-down resistors were used to stop floating input potential which might result in a LOW signal being sent during HIGH state.

A switch was used with the same functionality as a button without pull-down resistor. Buttons supply signals for Single step and reset while the switch supplies signal for continuous mode or stepping mode.

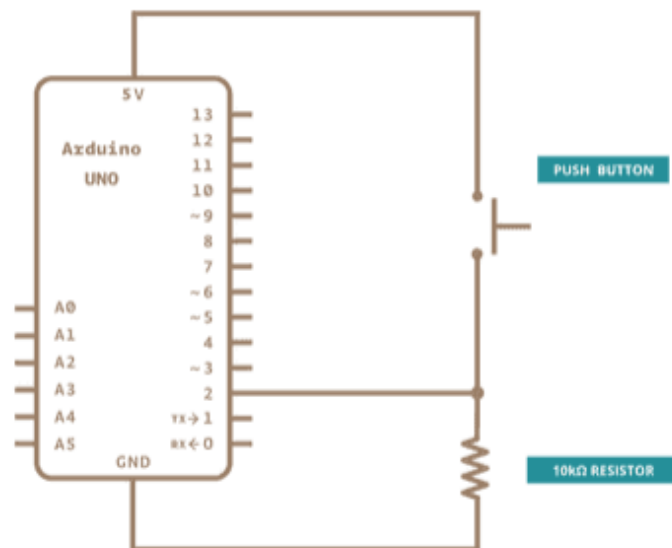


Figure 4.6.2: Schematic of a single button circuit. [\[11\]](#)

### The motor Circuit

The L298N is supplied by a 12V DC power supply unit and grounded with the arduino to create a signal loop.

This allows the arduino to drive a higher current stepper motor than it would be able to on its own.

4 digital outputs from the arduino sends the step sequence to the driver that forwards it to the motor. This energizes the coils around the stator to turn the rotor see [Figure 4.6.3](#).

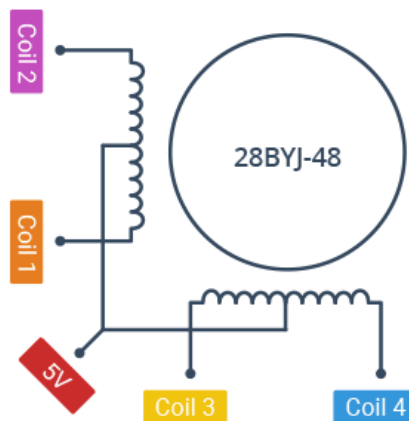


Figure 4.6.3: Different motor and supply voltage but same concept. [12]



Figure 4.6.4: The final control module

## 4.7 Programming Arduino

To be able to control the stepper motor the library AccelStepper was used to simplify the coding process. This allowed for precise control and greatly reduced time from manually coding the system.

The stepper motor had 200 steps per rotation this allowed for great precision. A variable named **STEPCOUNT** was set to update by 12.5 steps using half steps per button press to fit the 16 steps per rotation that was decided.

A WHILE loop depending on if the **RESET** button was pressed initiated the program. An IF statement depending on if the switch is HIGH or LOW activates what kind of stepping mode will be used between incremental step and continuous stepping.

For incremental steps the code runs an IF statement that activates when the **STEP** button is pressed, this enables the current to the motor, updates **STEPCOUNT** and rotates to the next position where after a short delay it disables the holding torque current.

When **STEPCOUNT** reaches the value 200 it rotates back to the origin position and resets the **STEPCOUNT** variable.

After every step the variable for step is increased and updates the output to the 7 segment display that reflects what step it is currently used.

Since there were two different displays one was needed to display 1-9 and since it would never use more than 17 different numbers it was unnecessary to use more numbers than 0 and 1 on the tens digit.

For continuous stepping the motor rotates with 10 step jumps without stopping simulating a continuous sweep of 360 degrees.

## 7. Conclusion

### 7.1 implementation of stepper motor control

Integrated automatic stepper motor control for the stirrer, enabling both incremental and continuous rotational functionalities. This provides the chamber with precise control over the tuner position. Using an Arduino with a program that is easy to update with new parameters if needed using the Arduino IDE software and libraries.

The necessity for constructing a new stirrer and deciding on keeping the existing one after testing the performance is evaluated.

### 7.2 Development of control Program

Designed and implemented a simple program to control and connect all test equipment associated with the chamber. This program simplifies testing procedures and significantly reduces test time compared to manual testing seeing how everything is automated, with no need to manually set each frequency and position.

The Pythonscript definitely has potential of improvement, since the script saves a single text file each time it runs a position that means it saves one script for 8 positions and 16 rotationsteps each totaling on 128 files which then is moved into excel to be analyzed. Being able to reduce these 128 test data files to 1 file or directly into excel would save even more time but this had to be cut to reduce time for the project.

### 7.3 Analysis according to standards

Conducted analysis of the RVC performance in accordance with MIL-461G And RTCA 160G standards.[\[1\]\[2\]](#)

In which the conclusion is that the chamber does not fit all requirements listed in the standards. This does not mean the chamber is unusable but it does mean that the deviations need to be listed and communicated with the customers to avoid misunderstandings.

The chamber frequency range was determined to be 1GHz to 18GHz, ensuring compatibility with testing requirements and standards.[\[1\]\[2\]](#)

The field uniformity was evaluated and both the Q-factor and the correlation to power output was measured and calculated providing insights into the chamber's performance.

The observed disparity between the measured Q factor and the Theoretical Q was notable. Despite the apparent magnitude of the difference, it actually falls within the anticipated range taken in consideration when evaluating the various potential sources of error.

Losses attributed to inefficient antenna performance, leakage losses and approximations made during calculations were all potential error sources. For instance, in the calculations the power was a fixed value of 0.03W instead of employing the accurate values measured for each position and frequency, thereby contributing to discrepancies in results. This all means that the resulting Q value is both expected and within acceptable range.

When calculating the calibration factor it was deemed the chamber could reach up to almost 350V/m with an input power of 1W compared to the roughly 1kW that would be needed in a semi-anechoic chamber to reach the same field strength. This is incredibly cost efficient and is believed to reduce the cost about 1000 times. The field strength in a semi-anechoic chamber was measured to about 3 magnitudes lower than the 350V/m the RVC can produce.

The field uniformity that was reached with the parameters of the performed test gave a field with  $X \text{ V/m} \pm 20\%$  which is perfectly acceptable.

In conclusion, the project was executed successfully and resulted in a significantly enhanced Reverberation Chamber. The implementation of stepper motor control coupled with the development of a comprehensive control program has greatly improved the RVC operational capabilities.

But it was also not able to meet all the requirements listed in the standard [\[1\]](#) so the customer has to be informed of the deviations from standard.

## References

[1] MIL-STD-461G, Department of defense interface standard

Requirement for the control of electromagnetic interference characteristics of subsystems and equipment.

Prepared by DoD agencies, Army, Navy, Airforce, December 11 2015.

[2] RTCA DO-160G , Environmental Conditions and Test Procedures for Airborne Equipment.

Prepared by RTCA SC-135 December 8, 2010.

[3] Introduction of randomness in deterministic, physically consistent descriptions of reverberation chambers and experimental verification. Published by Serra,R April 1, 2009.

[4] Statistical model for a mode-stirred chamber, IEEE Transactions on Electromagnetic Compatibility, Prepared by J. G. Kostas and B. Boverie 1991.

[5] Arduino UNO R3, <https://docs.arduino.cc/hardware/uno-rev3/>  
(Acc 2023-10-14)

[6] L298N Dual H bridge motor driver module. 13 april 2021, <https://components101.com/modules/l293n-motor-driver-module>  
(Acc 2023-10-14)

[7] Stepper motor, 2 april 2024, [https://en.wikipedia.org/wiki/Stepper\\_motor](https://en.wikipedia.org/wiki/Stepper_motor)  
(Acc 2023-10-14)

[8] Complete guide to stepper motors, 29 Augusti 2023, <https://uk.rs-online.com/web/content/discovery/ideas-and-advice/stepper-motors-guide>  
(Acc 2023-10-14)

[9] "Electromagnetic Reverberation Chambers: theory, uses, open questions and research" presented by Prof. Ramiro Serra, , Department of Electrical Engineering, Eindhoven University of Technology, The Netherlands. October 2, 2023

**[10] PyVISA the Python instrumentation package, 27 april 2023,**  
<https://joss.theoj.org/papers/10.21105/joss.05304#>  
**(Acc 2024-01-26)**

**[11] Digital read Serial, 8 December 2022,**  
<https://docs.arduino.cc/built-in-examples/basics/DigitalReadSerial/>  
**(Acc 2023-10-14)**

**[12] Control 28BYJ-48 stepper motor, 5 june 2020,**  
<https://lastminuteengineers.com/28byj48-stepper-motor-arduino-tutorial/>  
**(Acc 2023-10-14)**